HHS Public Access

Author manuscript

Neuroradiology. Author manuscript; available in PMC 2018 August 17.

Published in final edited form as:

Neuroradiology. 2017 February ; 59(2): 135–145. doi:10.1007/s00234-016-1769-8.

Advanced MRI assessment to predict benefit of anti-programmed cell death 1 protein immunotherapy response in patients with recurrent glioblastoma

Lei Qin[1,2], **Xiang Li**[3,4], **Amanda Stroiney**[1,5], **Jinrong Qu**[3,4], **Jeffrey Helgager**[6], **David A. Reardon**[7,8], and **Geoffrey S. Young**[2,4]

[1]Department of Imaging, Dana-Farber Cancer Institute, Boston, MA, USA

[2]Department of Radiology, Harvard Medical School, Boston, MA, USA

[3]Department of Radiology, Affiliated Cancer Hospital of Zhengzhou University, Zhengzhou, Henan, China

[4]Department of Radiology, Brigham and Women's Hospital, 75 Francis Street, Boston, MA 02115, USA

[5]Department of Behavioral Neuroscience, College of Sciences, Northeastern University, Boston, MA, USA

[6]Department of Pathology, Brigham and Women's Hospital, Boston, MA, USA

[7]CenterforNeuro-Oncology, Dana-Farber Cancer Institute, 44 Binney Street, Boston, MA 02115, USA

[8]Department of Medicine, Harvard Medical School, Boston, MA, USA

Abstract

Introduction—We describe the imaging findings encountered in GBM patients receiving immune checkpoint blockade and assess the potential of quantitative MRI biomarkers to differentiate patients who derive therapeutic benefit from those who do not.

Methods—A retrospective analysis was performed on longitudinal MRIs obtained on recurrent GBM patients enrolled on clinical trials. Among 10 patients with analyzable data, bidirectional diameters were measured on contrast enhanced T1 (pGd-T1WI) and volumes of interest (VOI) representing measurable abnormality suggestive of tumor were selected on pGdT1WI (pGdT1 VOI), FLAIR-T2WI (FLAIR VOI), and ADC maps. Intermediate ADC (IADC) VOI represented voxels within the FLAIR VOI having ADC in the range of highly cellular tumor ($0.7–1.1 \times 10^{-3}$ mm^2/s) (IADC VOI). Therapeutic benefit was determined by tissue pathology and survival on trial. IADC VOI, pGdT1 VOI, FLAIR VOI, and RANO assessment results were correlated with patient benefit.

Correspondence to: David A. Reardon; Geoffrey S. Young.

LQ and XL contributed equally to this work.

Electronic supplementary material The online version of this article (doi:10.1007/s00234-016-1769-8) contains supplementary material, which is available to authorized users.

Results—Five patients were deemed to have received therapeutic benefit and the other five patients did not. The average time on trial for the benefit group was 194 days, as compared to 81 days for the no benefit group. IADC VOI correlated well with the presence or absence of clinical benefit in 10 patients. Furthermore, pGd VOI, FLAIR VOI, and RANO assessment correlated less well with response.

Conclusion—MRI reveals an initial increase in volumes of abnormal tissue with contrast enhancement, edema, and intermediate ADC suggesting hypercellularity within the first 0–6 months of immunotherapy. Subsequent stabilization and improvement in IADC VOI appear to better predict ultimate therapeutic benefit from these agents than conventional imaging.

Keywords

Immunotherapy; GBM; ADC; MRI; Pseudoprogression

Background

Glioblastoma (GBM) is the most common malignant primary brain tumor, with over 10,000 cases diagnosed in the USA each year [1]. Current gold-standard treatment with surgery, radiation, and chemotherapy has modestly improved 2 year survival but 5-year survival remains less than 10% [2].

Immunotherapies comprise several promising novel strategies for GBM treatment. The use of blocking antibodies against cytotoxic T lymphocyte-associated protein 4 (CTLA4) and programmed cell death 1 protein (PD-1) to inhibit these immune checkpoints has shown benefit in other cancers [3, 4] and in orthotopic GBM models [5–7]. As immune checkpoint inhibitors enter clinical trials in recurrent as well as newly diagnosed GBM patients, there is an urgent need to understand the MRI changes induced by these agents in order to reliably assess the efficacy of these treatments [8]. Experience with anti-CTLA4 (ipilimumab) immunotherapy in non-CNS tumors has demonstrated different patterns of enhancing tumor change on MRI compared to patients undergoing conventional cytotoxic therapy [9]. Specifically, MRI scans from some patients demonstrate an early increase in enhancing tumor size or development of new enhancing lesions followed by stabilization or decrease in enhancing tumor size later in the course of therapy [10].

Interpreting change in abnormality on conventional anatomic brain MRI contrast-enhanced T1 weighted imaging (pGd-T1WI) and Fluid Attenuated Inversion Recovery T2WI (FLAIR-T2WI) can be difficult because immunotherapeutics may produce an inflammatory response that leads to increased contrast enhancement and vasogenic edema. Such changes are referred to as “pseudoprogression” and may be indistinguishable radiographically from true tumor progression with conventional imaging. Guidelines to continuation of immunotherapy among neuro-oncology patients with initial progressive imaging findings pending confirmation of progression on follow-up imaging have recently been published as the immunotherapy response assessment in neuro-oncology (iRANO) criteria [9]. These criteria represent consensus recommendations developed by a multidisciplinary panel of neuro-oncology experts to achieve consistency among clinicians confronted by these challenging imaging findings. In some patients suspected of having progression, brain biopsy or

resection has been performed and histopathology findings consistent with treatment-induced inflammation have been observed [Reardon, unpublished data]. Other patients whose early clinical and/or imaging findings raise question of pseudo-progression may be observed with serial MRI during continuation of therapy for 6 months or more. Due to the morbidity, cost, and risk of brain biopsy and the short life expectancy of recurrent GBM patients, neither invasive sampling nor delayed surveillance follow-up is optimal. Early imaging biomarkers to reliably detect or predict response to immunotherapy are urgently needed to improve patient management and assessment of therapeutic efficacy.

Diffusion-weighted MRI (DWI) measurements of random thermal water motion can be used to characterize features of the microstructure of different tissues including tumor cellularity. Apparent diffusion coefficient (ADC) maps generated from DWI reveal significantly lower ADC in highly cellular tumor than in pseudoprogression [11, 12]. Lower ADC also has been shown to precede the development of new enhancing tumor on pGd-T1WI [13]. Also, ADC has been shown to correlate with tumor grade, cellularity, treatment efficacy, and clinical outcome in primary CNS lymphoma patients treated with immunochemotherapy [14]. Of note, very low ADC similar to that seen in infarction has been reported in necrosis, particularly in patients on angiogenesis inhibition therapy [19, 29]. As such, we hypothesize that changes in the volume of tissue with intermediate ADC suggestive of highly cellular tumor (IADC VOI) may help assess and/or predict response to immune checkpoint therapy.

Methods

Patients

Fifteen consecutive patients enrolled in ongoing clinical trials (NCT02017717; NCT02054806) of anti-PD1 therapy (nivolumab, Bristol-Myers Squibb, Princeton, NJ, USA; and pembrolizumab, Merck, Kenilworth, NJ, USA) with or without anti-CTLA4 therapy (ipilimumab, Bristol-Myers Squibb, Princeton, NJ, USA) were included in this analysis. All patients enrolled in these trials had a histologically confirmed recurrence of Grade IV malignant glioma after radiotherapy (RT) and temozolomide (TMZ) with at least one clearly defined measurable enhancing lesion according to response assessment in neuro-oncology (RANO) [15] criteria and no surgery or treatment in the 4 weeks prior to starting the trial. All patients were at least 3 months from any prior radiotherapy and none had received any previous immunotherapy or anti-angiogenic therapy. None of the patients were on more than 4 mg of dexamethasone or an increasing dose of dexametha-sone at the time of study enrollment. Patients on these trials were treated with standard dose levels of these agents every 2 weeks until progressive disease, unacceptable toxicity, or withdrawal of consent. Assessment of outcome was determined by the treating clinician for these trials.

Patients on trial <2 months at the time of analysis were excluded since too few MRI data points were available for analysis.

MRI acquisition

MR data acquired during trial on 1.5 or 3T scanners (HDx/Excite/MR750w produced by GE Healthcare, Waukesha, WI; or Tim Aera/Trio/Verio/Skyra produced by Siemens Erlangen,

Germany) was retrieved for analysis including axial FLAIR T2WI (TR/TE/TI = 8000–12,550/81–135/2000–2650 ms; slice thickness/gap 3–5/0–1 mm; matrix 256–384 × 244–288), axial spin echo precontrast and post-contrast T1WI (TR/TE = 400–706/2.5–17 ms; slice thickness/gap 3–5/0– 1 mm; matrix 256–384 × 192–244), axial single shot spin echo echo-planar imaging DWI(TR/TE 6000–10,000/82–98 ms; b = 0,1000 s/mm^2; slice thickness/gap 5/1 mm; matrix 96–192 × 128–192). ADC maps were calculated using the software supplied by the MRI system manufacturer. Scans that did not have all three sequences were excluded from the study.

Image post-processing and volume measurement

The last scan prior to initiation of study therapy was defined as the baseline. Scans were co-registered and resampled bilinearly to the baseline post-contrast T1WI using commercial image processing software (Mirada(R), version 17.0, Chicago, IL, USA). Rigid registration was applied initially. If a change in brain anatomy since baseline related to an increase or decrease in edema and/or the tumor rendered the rigid registration unsuccessful, deformable registration was applied. If deformable registration was also unsuccessful, the MRI data were excluded. Correctness of image registration at each time point was determined by visual inspection by a qualified neuroradiologist with 10 years of experience.

To eliminate hyperintensity from hemorrhage on post-contrast images and highlight contrast enhancement, precontrast T1WI were subtracted from post-contrast T1WI using a commercial image processing workstation (Hermes(R) Hybrid Viewer, Hermes Medical solutions, Stockholm, Sweden) [16] (Fig. 1a). Detectably abnormal tissue was selected manually on each section by a neuroradiologist, and the area of abnormality was summed to create a volume of interest (VOI) representing the amount of abnormal tissue on subtracted contrast-enhanced T1WI (pGd-T1 VOI) and FLAIR T2WI (FLAIR VOI). The FLAIR VOI was then copied to the corresponding registered ADC maps. The volume of tissue within the FLAIR VOI having intermediate ADC in the range of 0.7–1.1 × 10^{-3} mm^2/s (IADC VOI) was included as a potential marker of solid tumor tissue [17–19] (Fig. 1b). To minimize the effects of registration error between FLAIR T2WI and ADC, and reduce partial volume averaging effects on the ADC maps, pixels within 5 pixels of the boundary on each section were excluded.

The relative change in volume of abnormal tissue FLAIR T2WI, pGdT1WI, and ADC maps was calculated as percentage change from baseline. A volumetric change of ≥25% was classified as an increase or decrease. Volume changes of 0–25% were classified as stable. As per RANO [15], percent change was used rather than absolute volumetric change in order to produce a metric of tumor growth that was comparable between patients with different amounts of detectable abnormality on baseline MRI [15]. When there is minimal or no detectable abnormality on the baseline MRI, this method artifactually amplifies small variations in tumor measurement. To compensate for this and to apply this to 3D volumetrics, we used a minimum volume of 1.0 cm^3 to define a measurable lesion (≥1.0 cm × 1.0 cm on axial images). We applied this threshold to all data types including ADC. In addition, we defined the minimum measurable change in volume as 1.0 cm^3. When

assessing change, calculated absolute volumes or change in volumes <1.0 cm^3 were disregarded.

As per RANO criteria [15], products of the perpendicular diameters of the lesions were determined on pGdT1WI. If there were multiple contrast-enhancing lesions, two largest lesions were measured, and the sum of the products was reported.

Analysis

Patients surviving on trial more than 5 months from the start of the clinical trial without unequivocal imaging, clinical, or histopathologic evidence of progression were classified as having received therapeutic benefit. Patients who experienced progression before 5 months on trial were deemed to not have received therapeutic benefit. Patients who underwent resection or biopsy during the trial because of imaging evidence of worsening edema and enhancement were classified as not having received significant benefit if the pathologic specimen revealed a predominance of active viable tumor, and as having received therapeutic benefit if the specimen revealed predominantly necrosis, inflammation, and/or other treatment-related effects. In order to assess potential confounding effects of corticosteroid dosing, steroid dose at the time of each MRI was recorded and temporally correlated with changes in MRI measures.

Results

Ten patients who met criteria for participation had analyzable data. Five patients achieved therapeutic benefit (“benefit” group) from immunotherapy. All five of these patients remained on trial for more than 5 months, and one of these patients had pathological confirmation of inflammatory treatment effect with necrosis, macrophage, and inflammatory cell infiltration and immature regenerative blood vessels (Fig. 2). Five patients were deemed not to have received therapeutic benefit from the treatment (“no benefit” group). All of these patients had been removed from the trial for clinically worse symptoms, progressive imaging findings or underwent surgery with pathology revealing extensive viable tumor. As expected, patients in the benefit group received immunotherapy significantly longer (194 days on average) than those in the no benefit group (81 days) (Table 1). Patients 8, 9, and 10 continued to receive study therapy at the cutoff for this analysis.

Although IADC VOI transiently worsened in some patients, it ultimately decreased for all patients in the therapeutic benefit group (patients 6–10). In contrast, IADC VOI ultimately increased progressively in all patients in the no benefit group (patients 1–5) with measurable disease, regardless of changes in RANO measures, pGd-T1 VOI, FLAIR-VOI, or corticosteroid dosing. Volumetric IADC change seems to correlate better with treatment benefit than volumetric change in pGd-T1WI or FLAIR-T2WI, or change in 2D RANO cross product measurements. In 3/10 patients (2/5 FP & 1/5 FN), change in 2D RANO measurements did not match the clinical outcome (patients 2, 4, 6). In 3/10 patients (1/5 FP & 2/5 FN), change in pGd-T1 VOI did not match the clinical outcome (patients 2, 6, 8). In 2/10 patients (2/5 FP & 0/5 FN), change in FLAIR VOI did not correlate with patient benefit (patients 2, 4). Although change in FLAIR VOI performed better than RANO measurements or pGd-T1 VOI, it was not as accurate as change in IADC VOI which correlated with patient

benefit in all 10/10 cases (0/5 FP & 0/5 FN). Figures 3 and 4 show typical cases from the two groups.

IADC VOI and FLAIR VOI began to decrease from 0 to 175 days (93 ± 59 days) and 0 to 220 days (121 ± 71 days), respectively, after start of immunotherapy in the patients who received significant benefit (Table 1).

Discussion

Introduction of temozolomide chemoradiation (TMZ-RT), angiogenesis inhibition (AI), and now immunotherapy (IT) have significantly reduced the usefulness of relying solely on the assessment of contrast enhancing tumor to predict response among malignant glioma patients. The RANO criteria for assessment of response in GBM is based on change in pGd-T1WI, similar to RECIST criteria in other cancers, with the addition of criteria for change on FLAIR-T2WI to account for the prominent nonenhancing component of many GBM tumors [20, 21]. TMZ-RT produces early abnormal enhancement and edema termed “pseudoprogression” in roughly 20% of patients which represents a combination of necrosis, infarction, and inflammation that mimics tumor progression on pGd-T1WI and FLAIR-T2WI [22]. AI can suppress enhancement in solid tumor and edema in infiltrative tumor [23]. The effects of IT on MR markers of tumor progression remain to be fully defined but seem to include early increase in contrast enhancement and edema in animal models which are thought to represent immune-mediated inflammation and/or necrosis [24].

A number of physiologic MRI techniques are under active investigation in an attempt to improve the accuracy of detection of tumor progression among malignant glioma patients, particularly with regard to patients who may have TMZ-RT pseudoprogression and AI pseudo-response. DWI, included in our study, is one of the most promising techniques. DWI allows semiquantitative estimation of the relative mixture of extracellular and intracellular/membrane-associated water in tissue by assaying the relative freedom of thermal movement of water. The high cellularity of malignant glial tumors should exert an opposite effect on average voxel ADC from the prominent extracellular edema expected with inflammation and the decreased cellularity expected with necrosis. Pretreatment ADC has been demonstrated to predict overall survival in high-grade glioma patients [25] and to determine true progression after tumor resection, TMZ-RT [11, 26], or AI [27–29]. For this reason, we chose to focus on volume of abnormal tissue with intermediate ADC (IADC VOI) in this initial analysis of the imaging effects of immune checkpoint blockade in malignant glioma patients.

Prior literature on the use of ADC in brain tumors reports the use of a single ADC threshold to distinguish high ADC, due to low cellularity vasogenic edema and necrosis from intermediate ADC, due to high cellularity tumor [30]. In addition to typical high ADC necrosis, an additional form of necrosis—sometimes referred to as “gelatinous necrosis”—has been described, characterized by very low ADC in the area of necrosis [19, 29]. Often seen with angiogenesis inhibition, this gelatinous necrosis typically produces ADC much lower than the intermediate ADC of highly cellular glioma which persists for months before gradually resolving. In order to distinguish this low ADC necrosis from highly cellular

tumor, we employed two thresholds in our ADC analysis: an upper threshold above which voxels were classified as high ADC, due to edema/necrosis and a lower threshold below which voxels were classified as low ADC, due to gelatinous necrosis. The optimal ADC thresholds for differentiation of low and high grade glioma have been reported to be in the range 0.6–1.1 × 10^{-3} mm^2/s in the literature when a single discriminatory threshold is employed [17, 18, 31]. We selected 1.1 × 10^{-3} mm^2/s as our high ADC threshold to separate cellular tumor from high ADC due to vasogenic edema/infiltrative tumor edema and typical high ADC necrosis. Histologically proven gelatinous necrosis has been reported to have a very low ADC in the range of 0.593–0.637 × 10^{-3} mm^2/s [19]. Therefore, we selected 0.7 × 10^{-3} mm^2/s as our low ADC threshold to differentiate cellular tumor from gelatinous necrosis. We chose to use this lower ADC threshold as well as the conventional upper ADC threshold because of the possibility that inflammation/necrosis related to IT may cause low ADC necrosis, especially when combined with anti-angiogenic therapy. Although the resulting intermediate ADC volume (IADC VOI) may slightly decrease our sensitivity to detect cellular tumor, we believe that the overall accuracy will be improved by reducing erroneous classification of IT-induced necrosis as progressive tumor.

Applying these thresholds to brain MRI of recurrent GBM patients undergoing anti-PD1 ± anti-CTLA-4 treatment, we found that volumetric IADC VOI change (10/10 correct) over time seems to correlate better with treatment benefit than volumetric change in pGd-T1WI (7/10 correct) or FLAIR-T2WI (8/10 correct), and RANO measures (7/10 correct).

Patient 6 (Fig. 2) was determined to have progressive disease based on trial-mandated RANO criteria and underwent surgery on day 137. The pathology revealed only 10% tumor and a prominence of inflammatory infiltrate, which suggested that the patient was responding to the treatment, in accordance with the FLAIR VOI and IADC VOI change.

Increased corticosteroid dosing can decrease the permeability of tumor blood vessels leading to a decrease in measured volume of enhancing tumor and nonenhancing infiltrative tumor-edema which may confound assessment of response [32, 33]. Because of this, we recorded the daily steroid dose prior to initiating immune checkpoint therapy and at the time of each MRI. We then assessed for correlation between the change in steroid dose and the change of pGd-T1 VOI, FLAIR VOI, and IADC VOI (supplemental Table S1). Most patients (n = 7) did not increase their daily decadron dose while on study therapy. Among those who received an increased daily dose, only one patient who achieved significant benefit had an increment of increase greater than 3 mg: patient #7 who underwent a brief trial of higher decadron dosing as discussed below. In sum, although our analysis is limited by our small sample size, no consistent trend suggesting a substantial confounding steroid dosing effect was observed, but we cannot completely exclude the possibility of a confounding correlation. Further analysis in future larger datasets should help to clarify this issue.

Interpretation of imaging in patient 7 is complicated by change in steroid dosing with a significant increase in decadron dose on day 155 (see supplemental Table S1). Corticosteroids act to decrease blood-brain barrier permeability which likely contributes to the volumetric decrease in abnormality on FLAIR-T2WI and pGd T1WI. While this could also reduce the high ADC of infiltrative tumor-edema, in areas of densely cellular tumor

where the intermediate ADC reflects a low extracellular volume fraction, further decrease in the local BBB permeability would not be expected to have as significant an effect on ADC. The relative insensitivity of IADC tumor volume to steroid dosing is supported by our clinical experience as illustrated by the images of patient #2 (Fig. 4b). Subsequent imaging of patient #7 after completion of the trial on day #155 supports the interpretation that the imaging improvement represents in large part therapeutic benefit rather than simply steroid effect: By day 190 (45 days after the trial ended), corticosteroid dose had been decreased to half the day 155 dose, but IADC VOI and FLAIR VOI continued to decrease and pGdT1 VOI increased only slightly.

Our preliminary data derived from anti-PD1 treatment of recurrent GBM suggest that all three volumes can increase for the first 0 ~ 6 months even in patients who ultimately derive significant benefit. Although early increase in IADC-VOI has been demonstrated to correlate with worse response and survival in patients treated with XRT and chemoradiation [34], it does not seem to predict progression in anti-PD1 immunotherapy patients, at least in the first 6 months. Several possible explanations for this include (a) that immunotherapy may have a delayed onset of cytotoxic effect leading to continued growth of cellular tumor over several months and (b) that immunotherapy may initially produce an inflammatory cell swelling and macrophage and other inflammatory cell infiltration that decreases ADC. Further investigation in animal models is needed as well as analysis of a larger sample of IT patients. In addition, this initial apparent worsening of MRI abnormality in all patients raises the possibility that some patients who discontinued treatment early might have benefitted if they had remained on treatment longer. The use of anti-PD1 IT combined with angiogenesis inhibition to reduce the effects of IT-induced inflammation may help shed light on this possibility. Also of note, all three patients who received combined anti-PD1 and anti-CTLA4 drugs were in the benefit group with a survival of at least 8 months (244–320 days) from the start of immunotherapy, and two out of three patients continue on therapy at the time data were analyzed for this report. Whether this reflects improved tolerance of the therapy, improved efficacy or both warrant further investigation.

Conclusions

Preliminary data from advanced MRI assessment suggests that increase in volume of abnormal tissue with contrast enhancement, edema, and intermediate ADC occurs in most patients during the initial months of anti-PD1 ± anti-CTLA-4 immunotherapy. Among patients who appear to achieve therapeutic benefit, subsequent improvement in these MRI markers was observed. Our findings suggest that volumetric change in IADC VOI may correlate better with therapeutic benefit than RANO criteria measures, pGdT1WI volumetrics, or FLAIR-T2WI volumetrics. Further investigation in animal models and analysis of a larger human trial dataset is indicated to confirm these findings, to more precisely define the relevant time course of this early immunotherapy-induced pseudoprogression and to investigate underlying mechanisms.

Supplementary Material

Refer to Web version on PubMed Central for supplementary material.

Acknowledgments

We thank Annie G. Bryant, Northeastern University, for assistance with the manuscript preparation and submission.

DAR reports personal fees from AbbVie, personal fees from Bristol Myers Squibb, personal fees from Cavion, grants and personal fees from Celldex, personal fees from Genentech Roche, grants and personal fees from Inovio, personal fees from Juno Pharmaceuticals, personal fees from Merck, grants and personal fees from Midatech, personal fees from Momenta Pharmaceuticals, personal fees from Novartis, personal fees from Novocure, personal fees from Oxigene, personal fees from Regeneron, personal fees from Stemline Therapeutics, and grants from Incyte, outside the submitted work

References

1. DeAngelis LM, Wen PY. Primary and metastatic tumors of the nervous system. In: Longo DL, Kasper DL, Hauser SL, Jameson J, Loscalzo J, editorsHarrison's principles of internal medicine. 2012.
2. Avril T, Vauleon E, Tanguy-Royer S, Mosser J, Quillien V. Mechanisms of immunomodulation in human glioblastoma. Immunotherapy. 2011; 3:42–44. [PubMed: 21524170]
3. Wolchok JD, Kluger H, Callahan MK, et al. Nivolumab plus ipilimumab in advanced melanoma. N Engl J Med. 2013; 369:122–133. [PubMed: 23724867]
4. Ansell SM, Lesokhin AM, Borrello I, et al. PD-1 blockade with nivolumab in relapsed or refractory Hodgkin's lymphoma. N Engl J Med. 2015; 372:311–319. [PubMed: 25482239]
5. Reardon DA, Gokhale PC, Klein SR, et al. Glioblastomaeradication following immune checkpoint blockade in an orthotopic, Immunocompetentmodel. Cancer Immunol Res. 2016; 4:124–135. [PubMed: 26546453]
6. Zeng J, See AP, Phallen J, et al. Anti-PD-1 blockade and stereotactic radiation produce long-term survival in mice with intracranial gliomas. Int J Radiat Oncol Biol Phys. 2013; 86:343–349. [PubMed: 23462419]
7. Wainwright DA, Chang AL, Dey M, et al. Durable therapeutic efficacy utilizing combinatorial blockade against IDO, CTLA-4, and PD-L1 in mice with brain tumors. Clin Cancer Res. 2014; 20:5290–5301. [PubMed: 24691018]
8. Reardon DA, Ballman KV, Buckner JC, Chang SM, Ellingson BM. Impact of imaging measurements on response assessment in glioblastoma clinical trials. Neuro-Oncology. 2014; 16(Suppl 7):vii24–vii35. [PubMed: 25313236]
9. Okada H, Weller M, Huang R, et al. Immunotherapy response assessment in neuro-oncology: a report of the RANO working group. The Lancet Oncology. 2015; 16:e534–e542. [PubMed: 26545842]
10. Wolchok JD, Hoos A, O'Day S, et al. Guidelines for the evaluation of immune therapy activity in solid tumors: immune-related response criteria. Clin Cancer Res. 2009; 15:7412–7420. [PubMed: 19934295]
11. Chu HH, Choi SH, Ryoo I, et al. Differentiation of true progression from pseudoprogression in glioblastoma treated with radiation therapy and concomitant temozolomide: comparison study of standard and high-b-value diffusion-weighted imaging. Radiology. 2013; 269:831–840. [PubMed: 23771912]
12. Vrabec M, Van Cauter S, Himmelreich U, et al. MR perfusion and diffusion imaging in the follow-up of recurrent glioblastoma treated with dendritic cell immunotherapy: a pilot study. Neuroradiology. 2011; 53:721–731. [PubMed: 21107549]
13. Gupta A, Young RJ, Karimi S, et al. Isolated diffusion restriction precedes the development of enhancing tumor in a subset of patients with glioblastoma. AJNR Am J Neuroradiology. 2011; 32:1301–1306.
14. Wieduwilt MJ, Valles F, Issa S, et al. Immunochemotherapy with intensive consolidation for primary CNS lymphoma: a pilot study and prognostic assessment by diffusion-weighted MRI. Clin Cancer Res. 2012; 18:1146–1155. [PubMed: 22228634]

15. Wen PY, Macdonald DR, Reardon DA, et al. Updated response assessment criteria for high-grade gliomas: response assessment in neuro-oncology working group. J Clin Oncol. 2010; 28:1963–1972. [PubMed: 20231676]
16. Ellingson BM, Kim HJ, Woodworth DC, et al. Recurrentglioblastoma treated with bevacizumab: contrast-enhanced T1-weighted subtraction maps improve tumor delineation and aid prediction of survival in a multicenter clinical trial. Radiology. 2014; 271:200–210. [PubMed: 24475840]
17. Porto L, Jurcoane A, Schwabe D, Kieslich M, Hattingen E. Differentiation between high and low grade tumours in paediatric patients by using apparent diffusion coefficients. Eur J Paediatr Neurol. 2013; 17:302–307. [PubMed: 23273960]
18. Kralik SF, Taha A, Kamer AP, Cardinal JS, Seltman TA, Ho CY. Diffusion imaging for tumor grading of supratentorial brain tumors in the first year of life. AJNR Am J Neuroradiol. 2014; 35:815–823. [PubMed: 24200900]
19. LaViolette PS, Mickevicius NJ, Cochran EJ, et al. Precise ex vivo histological validation of heightened cellularity and diffusion-restricted necrosis in regions of dark apparent diffusion coefficient in 7 cases of high-grade glioma. Neuro-Oncology. 2014; 16:1599–1606. [PubMed: 25059209]
20. Kumar AJ, Leeds NE, Fuller GN, et al. Malignantgliomas: MR imaging spectrum of radiation therapy- and chemotherapy-induced necrosis of the brain after treatment. Radiology. 2000; 217:377–384. [PubMed: 11058631]
21. Ulmer S, Braga TA, Barker FG 2nd, Lev MH, Gonzalez RG, Henson JW. Clinical and radiographic features of peritumoral infarction following resection of glioblastoma. Neurology. 2006; 67:1668–1670. [PubMed: 17101902]
22. Kruser TJ, Mehta MP, Robins HI. Pseudoprogression after glioma therapy: a comprehensive review. Expert Rev Neurother. 2013; 13:389–403. [PubMed: 23545054]
23. Hygino da Cruz LC, Rodriguez I, Domingues RC, Gasparetto EL, Sorensen AG. Pseudoprogression and pseudoresponse: imaging challenges in the assessment of Posttreatmentglioma. Am J Neuroradiol. 2011; 32:1978–1985. [PubMed: 21393407]
24. Reardon DA, Gokhale PC, Klein SR, et al. Glioblastomaeradication following immune checkpoint blockade in an orthotopic, Immunocompetentmodel. Cancer Immunol Res. 2015; 4:124–135. [PubMed: 26546453]
25. Hilario A, Sepulveda JM, Perez-Nunez A, et al. A prognostic model based on preoperative MRI predicts overall survival in patients with diffuse gliomas. AJNR Am J Neuroradiol. 2014; 35:1096–1102. [PubMed: 24457819]
26. Prager AJ, Martinez N, Beal K, Omuro A, Zhang Z, Young RJ. Diffusion and perfusion MRI to differentiate treatment-related changes including pseudoprogression from recurrent tumors in high-grade gliomas with histopathologic evidence. AJNR Am J Neuroradiol. 2015; 36:877–885. [PubMed: 25593202]
27. Nagane M, Kobayashi K, Tanaka M, et al. Predictive significance of mean apparent diffusion coefficient value for responsiveness of temozolomide-refractory malignant glioma to bevacizumab: preliminary report. Int J Clin Oncol. 2014; 19:16–23. [PubMed: 23354833]
28. Chen C, Huang R, MacLean A, et al. Recurrent high-grade glioma treated with bevacizumab: prognostic value of MGMT methylation, EGFR status and pretreatment MRI in determining response and survival. J Neuro-Oncol. 2013; 115:267–276.
29. Mong S, Ellingson BM, Nghiemphu PL, et al. Persistent diffusion-restricted lesions in bevacizumab-treated malignant gliomas are associated with improved survival compared with matched controls. AJNR Am J Neuroradiol. 2012; 33:1763–1770. [PubMed: 22538078]
30. Yamasaki F, Sugiyama K, Ohtaki M, et al. Glioblastoma treated with postoperative radio-chemotherapy: prognostic value of apparent diffusion coefficient at MR imaging. Eur J Radiol. 2010; 73:532–537. [PubMed: 19250783]
31. Yamasaki F, Kurisu K, Satoh K, et al. Apparent diffusion coefficient of human brain tumors at MR imaging. Radiology. 2005; 235:985–991. [PubMed: 15833979]
32. Watling CJ, Lee DH, Macdonald DR, Cairncross JG. Corticosteroid-induced magnetic resonance imaging changes in patients with recurrent malignant glioma. J Clin Oncol. 1994; 12:1886–1889. [PubMed: 8083712]

33. Goh JJ, See SJ, Ang E, Ng WH. Vanishing glioblastoma after corticosteroid therapy. J Clin Neurosci. 2009; 16:1226–1228. [PubMed: 19497751]

34. Elson A, Bovi J, Siker M, Schultz C, Paulson E. Evaluation of absolute and normalized apparent diffusion coefficient (ADC) values within the post-operative T2/FLAIR volume as adverse prognostic indicators in glioblastoma. J Neuro-Oncol. 2015; 122:549–558.

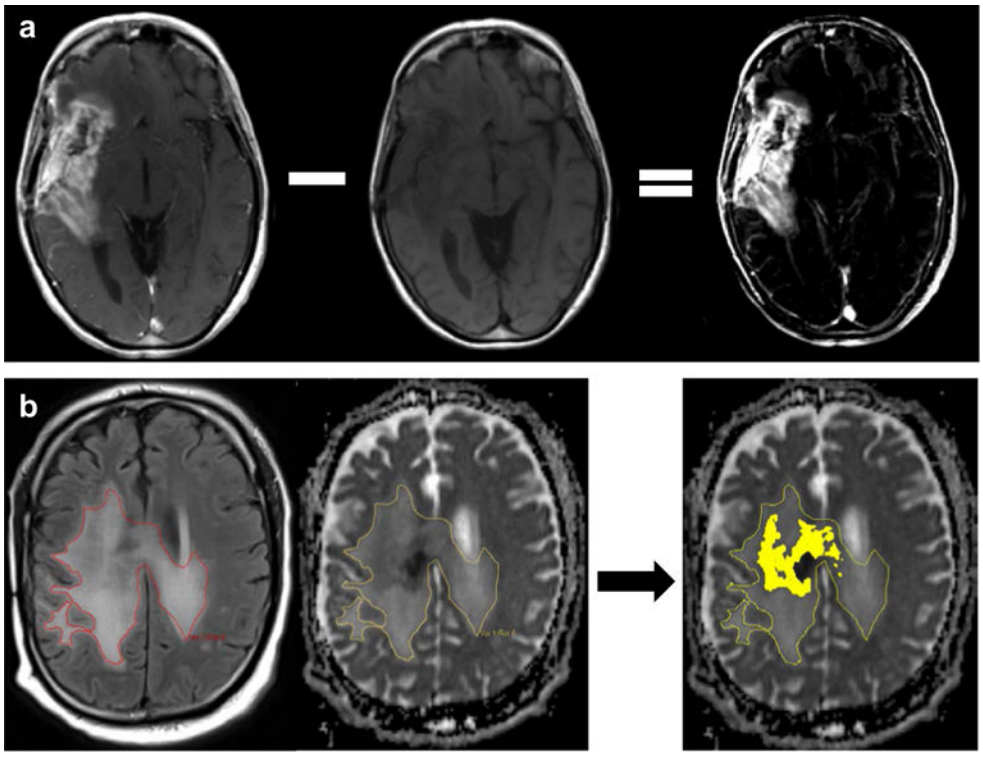

Fig.1.

a Pre- and post-Gd T1WI subtraction highlights the lesion in the subtracted T1 image. **b** ROI copied from FLAIR to ADC, and threshold of intermediate ADC (0.7–1.1) × 10^{-3} mm^2/s was applied inside the ROI. Volume measured from ADC map is the *yellow region* inside the ROI

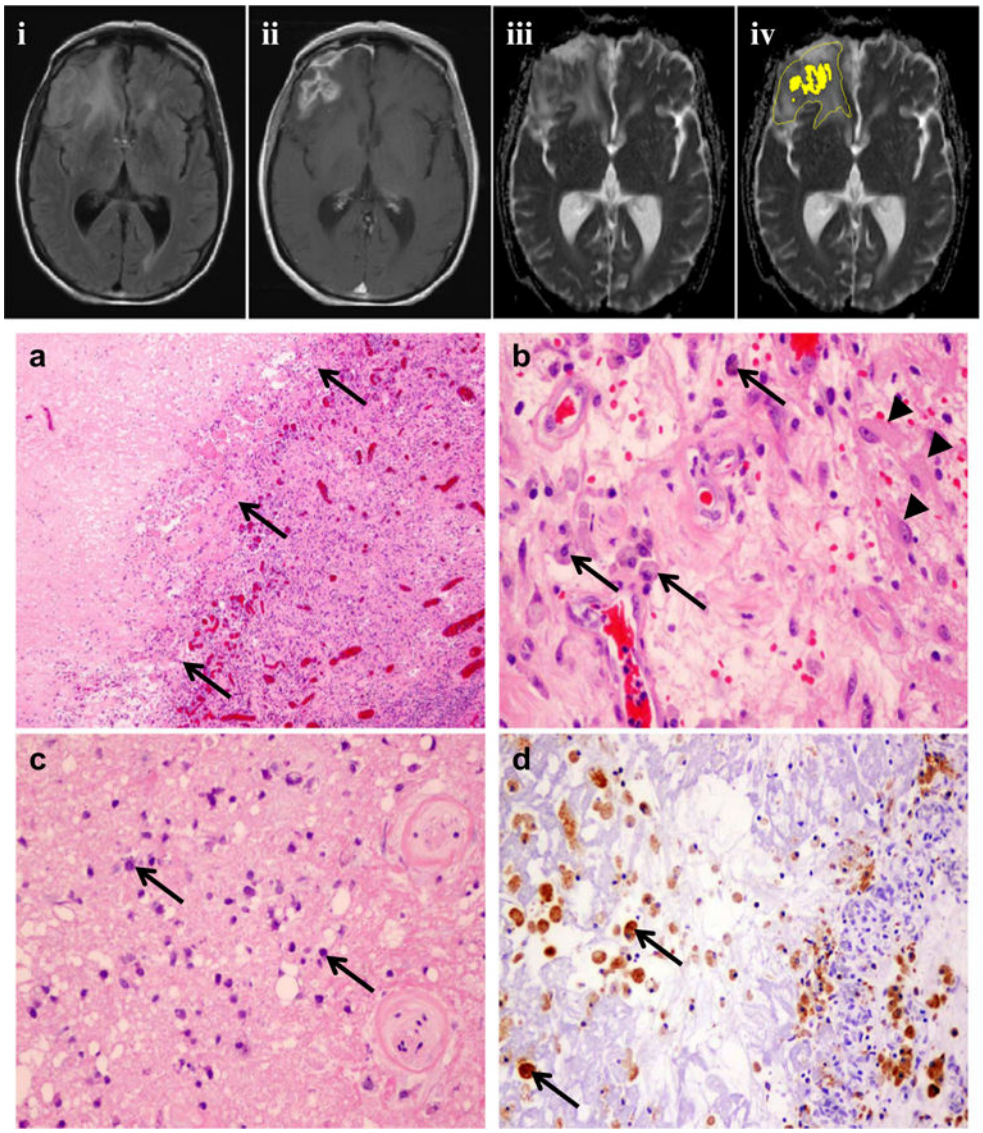

Fig. 2.

Patient #6 from Table 1. Preoperative axial MR images (*top row*) of the area of treated tumor that was subsequently biopsied include: (*i*) FLAIR T2WI demonstrating vasogenic edema, (*ii*) pGd T1WI demonstrating abnormal enhancement due to high vascular permeability, (*iii*) ADC map demonstrating predominantly high ADC suggestive edema and necrosis admixed with infiltrative tumor, and (*iv*) ADC map with IADC area segmented in yellow suggesting a small central area of cellular tumor. Histopathologic images from biopsy (*middle and bottom row*) include: **a** Low-power field of area of treated tumor showing a large swath of geographic necrosis (*left of arrows*), bordered by granulation tissue (*right of arrows*). Tumor cells are admixed; **b** high-power field of granulation tissue highlighting treatment effects including macrophages (*arrows*) with scattered admixed reactive astrocytes (*arrowheads*) in a background of newly formed blood vessels and edematous stroma, **c** high-power field of area of geographic necrosis showing scattered tumor cells (*arrows*), and **d** astain for CD68 highlighting numerous macrophages (*brown*, *arrows*), phagocytosing necrotic debris

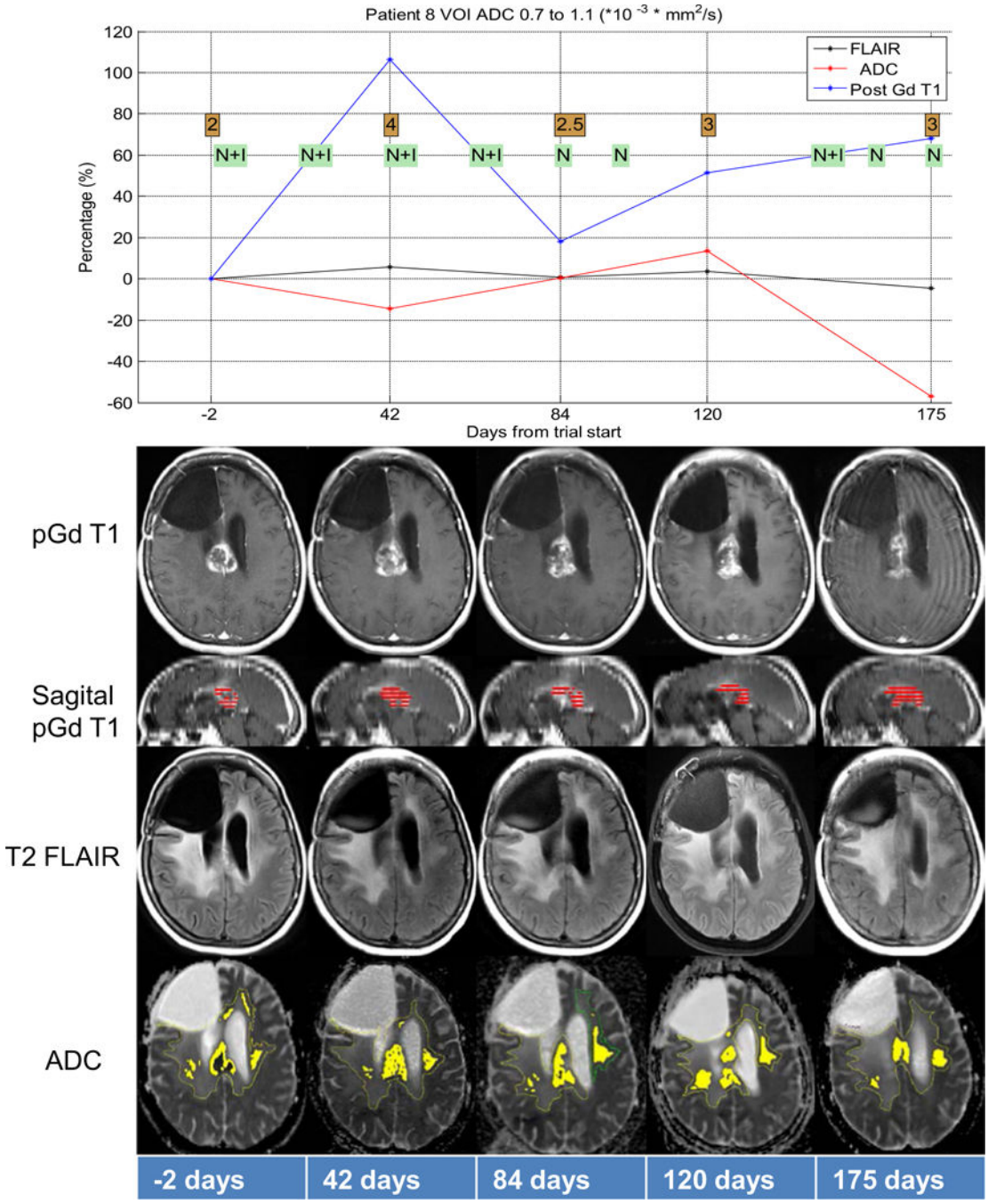

Fig. 3.

Representative significant benefit patient (patient # 8 from Table 1). On the graph, *green highlighted letters* indicate dates of Nivolumab(N) and Ipilumumab (I) dosing. The brown highlighted numbers indicate the decadron dose (mg/day). ADC volume begin to decrease between day 120 ~ 175. Corresponding MRI images illustrated below include pGd-T1WI axial and sagittal images in the top two rows, FLAIR-T2WI in the third row, and ADC in the bottom row. The sagittal images with the selected VOI shown in red are included to illustrate that pGd enhancing tumor volume decreases from day 42–84 and increases from day 120–

175 although this is not as apparent on the axial sections due to the unusual shape of the tumor

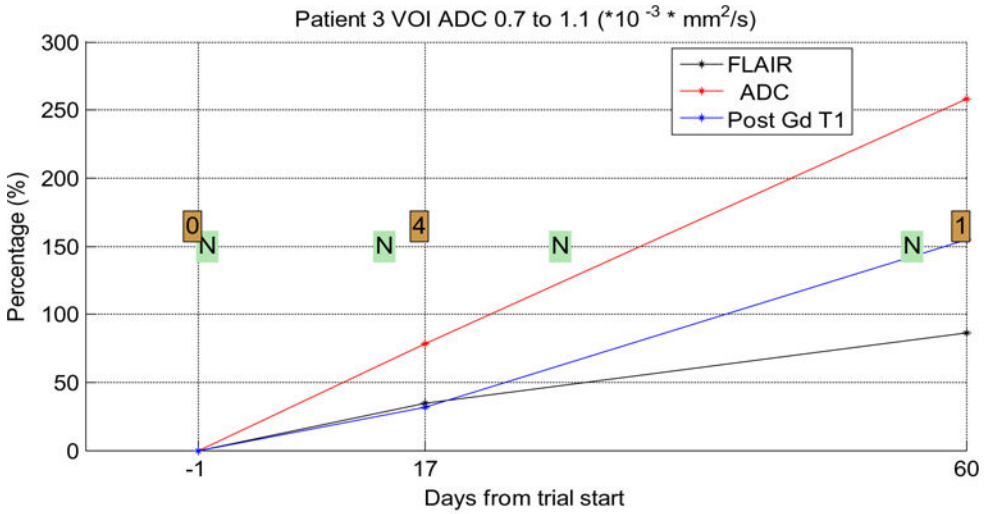

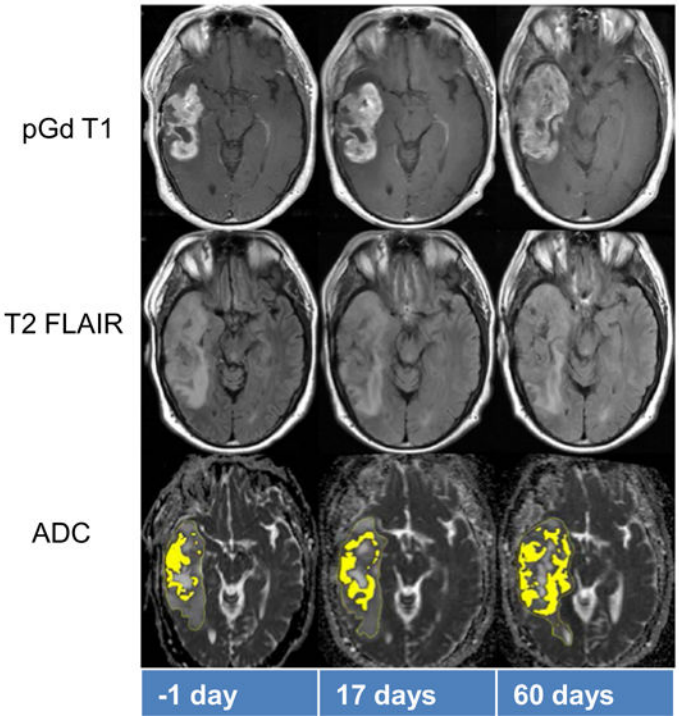

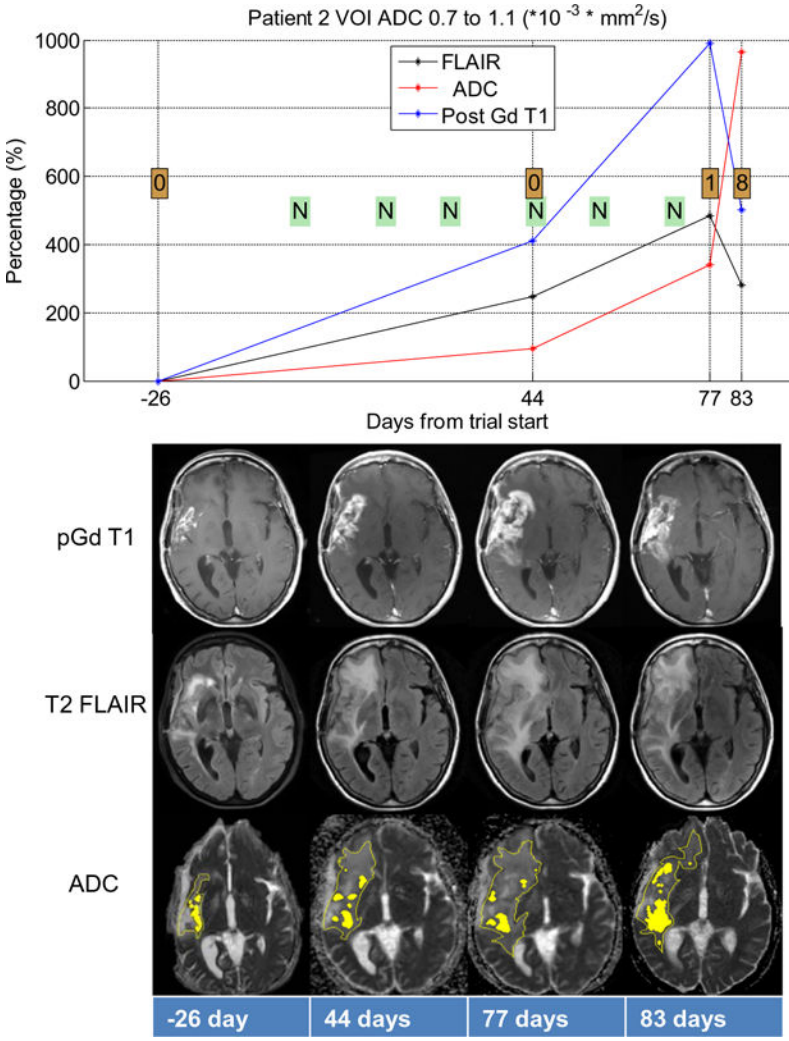

Fig. 4.

a Representative no clinical benefit patient (patient # 3 from Table 1). On the graph, *green highlighted letters* indicate dates of Nivolumab (N). The *brown highlighted numbers* indicate the decadron dose (mg/day). Corresponding MRI images illustrated below include pGd-T1WI (upper), FLAIR-T2WI (*middle*), and ADC (*lower*) panels. **b** Representative no clinical benefit patient demonstrating utility of ADC in setting of increasing corticosteroid dose (patient # 2 from Table 1). On the graph, the green highlighted letters indicate dates of Nivolumab (N). The brown highlighted numbers indicate the decadron dose (mg/day). Corresponding MRI images illustrated below include pGd-T1WI (*upper*), FLAIR-T2WI (*middle*), and ADC (*lower*) panels. The large increase in decadron dose on day 83 likely accounts for the substantial decrease in volume of abnormal enhancement on pGd T1 and edema on FLAIR T2WI, despite worsening clinical status. Although steroids may increase the rate of growth of the abnormal ADC volume, this continuing ADC volume increase is likely in large part due to tumor growth and helps to distinguish this steroid induced "pseudoresponse" from true therapeutic improvement in which abnormal ADC volume decreases

Table 1

Change in imaging markers including pGdTlWI RANO measures, FLAIR T2 VOI, pGd T1 VOI, and IADC VOI during immunotherapy

Pt	Treatment	Histo-pathologic findings	Time on Trial (days)	Decadron Dose (mg)	Significant Treatment Benefit?	RANO 2D	FLAIR volume	Post-Gd T1 volume	ADC volume	Days FLAIR starts to decrease?	Days ADC starts to decrease
1*	anti-PD1	1) 35% Tumor 2) 65% Tumor	84	→	No	TN	TN	TN	TN	NA	NA
2	anti-PD1	50% Tumor	84	↗	No	FP	FP	FP	TN	77~83	NA
3	anti-PD1	>50% Tumor	66	↘	No	TN	TN	TN	TN	NA	NA
4	anti-PD1	50% Tumor	114	↘	No	FP	FP	TN	TN	NA	NA
5	anti-PD1	>80% Tumor	56	↗	No	TN	TN	TN	TN	NA	NA
6	anti-PD1	10% Tumor	275	→	Yes	FN	TP	FN	TP	163 ~ 220	56 ~ 86
7	anti-PD1+ anti-CTLA4	NA	155	↗	Yes	TP	TP	TP	TP	141 ~ 155	141 ~ 155
8	anti-PD1+ anti-CTLA4	NA	189**	↗	Yes	TP	TP	FN	TP	NA	120 ~ 175
9	anti-PD1+ anti-CTLA4	NA	170**	→	Yes	TP NM+	TP	TP NM+	TP	84 ~ 156	0 ~ 42
10	anti-PD1	NA	182**	→	Yes	TP	TP	TP	TP	0 ~ 54	0 ~ 54

Decadron dosing, RANO measurements, and volume change in ADC, Post-Gd T1, and FLAIR VOI are in supplemental Table S1

TP/TN true positive/negative, imaging markers match clinical outcome in “benefit/no benefit” group, *FP/FN* false positive/negative, imaging markers do not match clinical outcome in “benefit/no benefit” group

*Pt 1 had 2 surgeries, performed on 90 and 119 days after immunotherapy respectively No anti-PD1 was given after surgery 1

**Patients who continue to receive study therapy at the cutoff for this analysis and the reported time on trial represents only the time from start of trial to date of analysis

+Lesion defined as nonmeasurable disease by RANO and our adapted criteria